Method for measurement of fusion-splicing-induced reflection in a photonic bandgap fiber-optical gyro

Xiaobin Xu (徐小斌)*, Zhihao Zhang (张智昊), Zuchen Zhang (张祖琛), Jing Jin (金 靖), and Ningfang Song (宋凝芳)

Institute of Opto-Electronics Technology, Beihang University, Beijing 100191, China

**Corresponding author: xuxiaobin@buaa.edu.cn*

Received September 27, 2014; accepted December 22, 2014; posted online February 27, 2015

We propose a method for the real-time measurement of the reflection at both splicing points between a photonic bandgap fiber coil and conventional fiber during the process of fusion splicing in a photonic bandgap fiber optical gyroscope (PBFOG), using the interference among the secondary waves, which arise from the fusion splicing points and the mirror face produced by intentionally cutting the bear end of the coupler. The method is theoretically proven and experimentally verified in a practical PBFOG, and it is significant for inline examination of the fusion splicing quality and evaluation of the PBFOG performance.

OCIS codes: 060.2310, 060.5295.

doi: 10.3788/COL201513.030601.

Photonic crystal fibers (PCFs) are characterized by a periodic arrangement of air holes around a core[1,2]. A photonic bandgap fiber (PBF) is a kind of air-core PCF, and it has attracted a great deal of interest owing to its unique optical properties[3,4]. A PBF makes the light propagate in air which is much more stable than SiO_2 in a conventional fiber, so it becomes a radically new method to solve the problems of environmental adaptability in a fiber-optical gyroscope (FOG). A FOG composed of a PBF coil is generally called a photonic bandgap fiber optical gyroscope (PBFOG), and a PBFOG has a greatly reduced sensitivity to the Kerr, irradiation, temperature transient, and Faraday effects compared to a conventional FOG[5,6].

Reflection occurs at an interface between two media exhibiting different refractive indices[7]. In a PBFOG, the pigtails of an integrated optic chip (IOC) or the succeeding Lyot depolarizers are conventional fibers which have a Ge-doped SiO_2 core, but the coil is made up of a PBF having an air core, as illustrated in Fig. 1. The strong reflection inevitably happens at both fusion splices between the PBF coil and the tail fibers of the IOC (or depolarizers)[8]. However, the reflectance is not always 4% as per the Fresnel law, because the endface of the fiber is not an ideal mirror face due to the damage of high temperature or imperfect cutting in the process of fusion splicing, as illustrated in Fig. 2. In fact, the reflectance may not even be a constant for each time of fusion splicing, because random fluctuation always exists for the fusion parameters such as power and cutting angle. In a PBFOG, the secondary waves reflected back to the detector can cause noise, even bias error if they are able to interfere when the length of the IOC tail fibers is not proper[7,9]. Therefore, it is extremely important to precisely measure the reflection at these two fusion splicing points, such that we can make an inline examination of the fusion splicing quality to control the reflection to an accepted level in time; the PBFOG performance can be evaluated with the measuring result of the reflection. In fact, reflection also exists in a conventional FOG, but it originates from the interfaces between the endfaces of the IOC and its tail fibers. A reflection of this kind is very small (<-60 dB), because the endfaces of both the IOC and its tail fibers are intentionally polished to some proper oblique angles to avoid the reflection[7,9]. Finally, the problems concerning the reflection can always be neglected in a conventional FOG, but it is a big problem in PBFOG. The traditional measuring methods, including optical time-domain reflectometer (OTDR) and optical continuous wave reflectometer (OCWR), are not feasible in this context due to the fact that it is a closed optical circuit in the sensing coil of the PBFOG[10]. In this Letter, we promote a simple method to implement inline measurement of the reflection at the splicing points between the PBF coil and the IOC tail fibers during the process of fusion splicing, without any alteration to the optical configuration of the PBFOG except replacement of the light source.

A scheme of measuring the reflection at fusion splicing points between the PBF coil and the pigtails of IOC is shown in Fig. 3[9]. The light outputs from the IOC pigtails with the power P_A and P_B (the subscripts A and B, throughout the paper, refer to Points A and B), and the corresponding secondary waves (W_A and W_B),

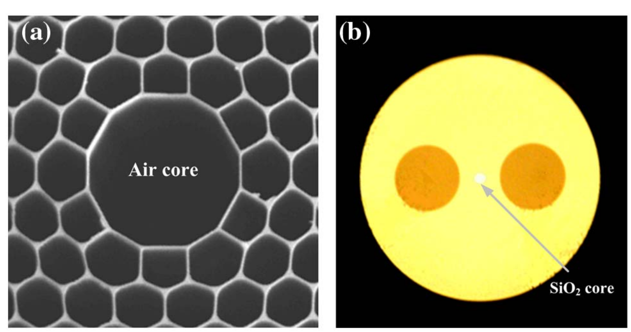

Fig. 1. Cross sections; (a) PBF; (b) conventional polarization-maintained fiber[11].

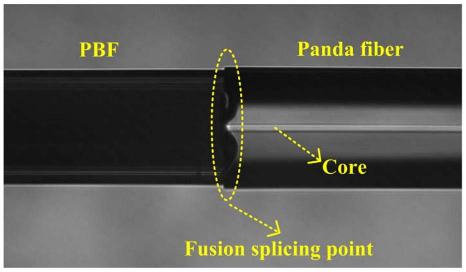

Fig. 2. Cross section of the fusion splicing point between the PBF and the conventional Panda fiber.

originate due to reflection at the interfaces. W_A and W_B go backward to the detector through the IOC and the coupler, respectively producing an intensity of V_A (mV) and V_B (mV) after photoelectronic conversion at the detector. The reflectance R, at Points A and B, is defined in this Letter as $R_A = V_A/(K_{\mathrm{PIN}}E_{\mathrm{PIN}}L_AP_A)$ and $R_B = V_B/(K_{\mathrm{PIN}}E_{\mathrm{PIN}}L_BP_B)$, respectively, where K_{PIN} and E_{PIN} are, respectively, the transimpedance and conversion efficiency of the detector which is always composed of a PIN photodiode and a field-effect transistor (FET); L_A and L_B are, respectively, the loss of the optical path from Points A and B to the detector. Those parameters are readily and accurately obtained except V_A and V_B, because V_A and V_B are not readily distinguished from the intensity produced by the clockwise (CW) and counter clockwise (CCW) primary waves (W_{CW} and W_{CCW}, Fig. 3) in a complete FOG. Therefore, V_A and V_B are actually our targets of measurement, which are crucial for the evaluation of fusion splicing quality and reflection-induced noise in a PBFOG.

The bear end of the coupler is intentionally cut to be a mirror face to produce another reflection-induced secondary wave W_C (the subscript C, throughout the paper, refers to Point C). W_C also goes backward to the detector through the coupler and produces an intensity of V_C (mV) at the detector. This artificial secondary wave provides some additional information and plays an important role in the process of measurement. A laser source with proper coherence length is employed to guarantee the interference among W_A, W_B, and W_C at the detector, but it must avoid the interference between the primary waves (W_{CW} and W_{CCW}) and the secondary waves (W_A, W_B, and W_C). A triangular wave with an amplitude of V_π and a period of T is applied to the IOC [Fig. 4(a)], and the modulation phase for W_A and W_B, is shown in Figs. 4(b) and 4(c), respectively. In this Letter, V_π is the half-wave voltage corresponding to the modulation phase of π (rad) for the light passing the upper branch of the IOC. In addition, W_C from the bear end of the coupler does not have any modulation phase because it never passes the IOC.

Before the fusion splicing of Points A and B, the intensity V_C must be measured at the detector. Then, splice the first point (Point A) through fusion; at the same time the endface of the other tail fiber of the IOC should be treated to avoid reflection and eliminate W_B. Thus only W_A and W_C exist, with the interference intensity of V_{AC} at the detector given by

$$V_{AC} = V_A + V_C + 2\sqrt{V_AV_C}\cos\left[\frac{4\pi}{T}t + \Phi_1(t)\right], \quad (1)$$

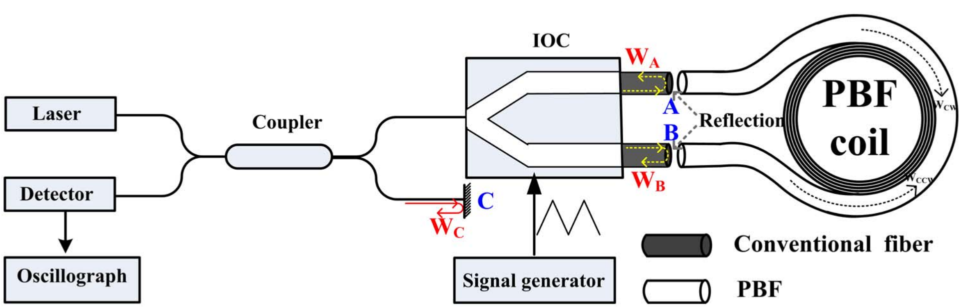

Fig. 3. Scheme of the measurement of fusion-splicing-induced reflection in a PBFOG.

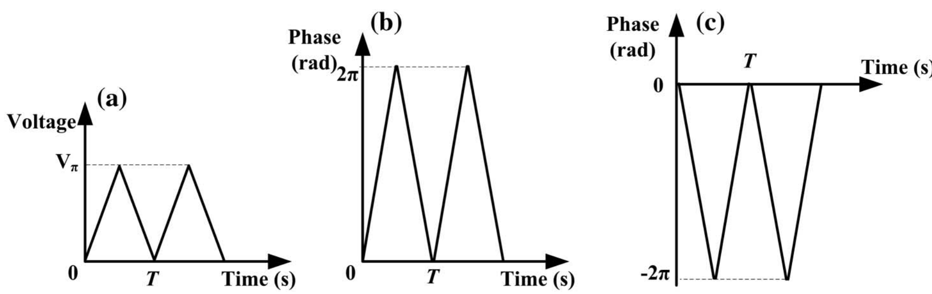

Fig. 4. (a) Modulation voltage applied on an IOC; (b) corresponding modulation phase for the secondary wave W_A; (c) corresponding modulation phase for the secondary wave W_B.

where t is time (nT to $nT + T/2$), V_{AC} is symmetric during the time $[nT + T/2$ to $(n+1)T]$, n is an integer, $\Phi_{m1}(t) = 4\pi t/T$ is the modulation phase for the interference signal, and $\Phi_1(t)$ is a random phase which varies with environment. Equation (1) indicates that the interference signal has a peak-to-peak (PTP) intensity ($V_{AC\text{-PTP}}$) of $4\sqrt{V_A}\sqrt{V_C}$ at the detector. Both the phase modulation and instability of the external environment cause the interference signal to vary with time, but $V_{AC\text{-PTP}}$ does not change. Moreover, $V_{AC\text{-PTP}}$ is easily measured as long as the modulation period T is small enough to make $\Phi_{m1}(t)$ vary faster than $\Phi_1(t)$. Consequently, the intensity V_A can be acquired as $V^2_{AC\text{-PTP}}/(16V_C)$.

In the next step, it is time to splice the other end (End B) of the PBF coil. The mirror face at the bear end of the coupler should be destroyed now to eliminate W_C, in order that only two secondary waves (W_A and W_B), and two primary waves (W_{CW} and W_{CCW}), exist at the detector during the process of this fusion splicing. As a result of the special choice of coherence length of the laser source, the interference only between W_A and W_B, and W_{CW} and W_{CCW}, can happen. The interference intensity between W_A and W_B at the detector is given by

$$V_{AB} = V_A + V_B + 2\sqrt{V_A V_B}\cos\left[\frac{8\pi}{T}t + \Phi_2(t)\right], \quad (2)$$

where the time t has the same definition as in Eq. (1), $\Phi_{m2}(t) = 8\pi t/T$ is the modulation phase for the interference signal, and $\Phi_2(t)$ is also a random phase which varies with the instable environment. Equation (2) shows that the interference signal (V_{AB}) has a PTP intensity ($V_{AB\text{-PTP}}$) of $4\sqrt{V_A}\sqrt{V_B}$ which can be directly measured at the detector. The intensity (V_B) is therefore resolved as $V^2_{AB\text{-PTP}}/(16V_A) = V_C V^2_{AB\text{-PTP}}/V^2_{AC\text{-PTP}}$. Note that the intensity of the interference between W_{CW} and W_{CCW} is a fixed value due to the fact that they are reciprocal (with the only phase difference being the Sagnac phase shift), so it merely causes a bias to V_{AB} and does not affect $V_{AB\text{-PTP}}$ when the PBF coil is in a static state.

An experimental setup has been established based on Fig. 3. A laser source with linewidth on the magnitude of megahertz (MHz) and power of ~0.425 mW is used to provide the coherent light. The coupler has a split ratio of ~50:50. The detector has a transimpedance of $K_{PIN} \sim 100$ kΩ and has a conversion efficiency of $E_{PIN} \sim 0.9$ A/W. The IOC is a kind of proton-exchange $LiNbO_3$ waveguide with half-wave voltage $V_\pi = \sim 5.1$ V. A triangular wave with an amplitude of V_π and period of $T \sim 10$ μs is applied to the IOC. Before splicing the PBF coil, we measure the output power from the IOC pigtails at Points A and B, and they are $P_A = 56.7$ μW and $P_B = 61.8$ μW. The bear end of the coupler is intentionally cut to be a mirror face and the secondary wave W_C is produced with the intensity (V_C) of ~690 mV at the detector. While we splice the first end (End A) of the PBF coil, the other end (End B) is kept immersed into the index-matching liquid to avoid reflection. As a result, there are only two large secondary waves (W_A and W_C) in the PBFOG. Their interference signal at the detector is shown in Fig. 5(a), indicating that the PTP intensity $V_{AC\text{-PTP}} \sim 312$ mV, so $V_A = V^2_{AC\text{-PTP}}/(16V_C) \sim 8.8$ mV, which corresponds to the reflectance of $R_A \sim 1.2\%$ based on the theory and experimental parameters mentioned previously. Then, we splice the other end (End B) of the PBF coil, and at the same time the mirror face at the bear end of the coupler is thoroughly destroyed to eliminate W_C. As a result, W_A interferes with W_B, and the interference intensity has a dependence on the modulation phase, as shown in Fig. 5(b). Obviously, its period (~2.5 μs) is a quarter of that of the modulation phase, and half of that of the interference signal between W_A and W_C [Fig. 5(a)], which agrees well with the theory. The PTP intensity $V_{AB\text{-PTP}} \sim 54$ mV, so $V_B = V_C V^2_{AB\text{-PTP}}/V^2_{AC\text{-PTP}} \sim 20$ mV, which corresponds to the reflectance of $R_B \sim 2.5\%$ at Point B. Therefore, strong reflection between the PBF coil and the tail fibers of the IOC indeed exists, and the reflectance seems not the same for each time of the fusion splicing possibly because of random

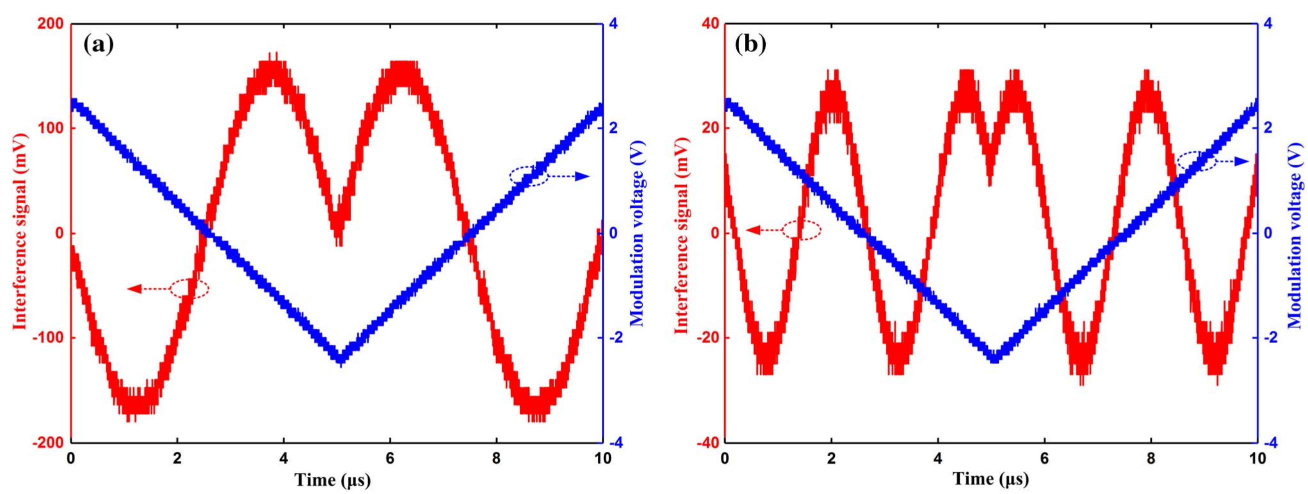

Fig. 5. Modulation voltage and interference signals; (a) between W_A and W_C; (b) between W_A and W_B.

fluctuation of the fusion power, cutting angle, interface shape, and so on.

The method provides a tool for inline monitoring of reflection at Points A and B during the process of fusion splicing, and its measurement precision depends to a large degree on the intensity of the secondary wave W_C. W_C actually serves as an amplifier to make the small W_A more easily measured, because the PTP intensity of the interference signal is $4\sqrt{V_C}\cdot\sqrt{V_A}$ while the End A of the PBF coil is being spliced and V_C is obviously much larger than V_A. If the noise of the interference signals at the detector is ΔV (to which many factors contribute such as shot noise, polarization noise, and scattering noise in a PBF), the precision of V_A is approximately $(\Delta V)^2/(16V_C)$. Therefore, a large V_C is very important to improve the measurement precision, but it should not be too large and cause the detector to be saturated. An increase of the reflectance at Interface C can be realized through some measures, such as attaching a short piece of fiber with angle-polished connector (APC)-type connector on one end and aluminum or gold coating at the other end, or temporarily covering the fiber end-face with liquid metal, although these measures are a little complex in the real-world process of fabricating a PBFOG.

On the other hand, if the reflection at Points A and B is so small that $V_{AB\text{-PTP}}$ cannot be measured during the process of splicing Point B, then we have to make some optimization to the method and let W_A, W_B, and W_C simultaneously exist at the detector. As a result, they interfere with each other and the interference intensity (V_{ABC}) is given by Eq. (3) with the omission of dc terms, where $\Phi_3(t)$ is also a random phase like $\Phi_1(t)$.

$$\begin{aligned} V_{ABC} = {} & 2\sqrt{V_A V_C}\cos\left[\frac{4\pi}{T}t+\Phi_1(t)\right] \\ & + 2\sqrt{V_B V_C}\cos\left[\frac{4\pi}{T}t+\Phi_3(t)\right] \\ & + 2\sqrt{V_A V_B}\cos\left[\frac{8\pi}{T}t+\Phi_2(t)\right]. \end{aligned} \tag{3}$$

In Eq. (3), $\sqrt{V_A}\sqrt{V_B}$ is significantly smaller than $\sqrt{V_A}\sqrt{V_C}$ or $\sqrt{V_B}\sqrt{V_C}$ when the V_C is large enough; therefore it can be neglected and the maximum PTP intensity ($V_{ABC\text{-PTP}}$) is $4(\sqrt{V_A}\sqrt{V_C}+\sqrt{V_B}\sqrt{V_C})$. As a result, $V_B \approx (V_{ABC\text{-PTP}} - V_{AC\text{-PTP}})^2/(16V_C)$ which can also be more accurate with larger V_C.

In conclusion, the reflection at the splicing points between the PBF coil and conventional tail fibers of IOC is an important factor affecting the precision and long-term stability of PBFOG. To precisely measure this reflection during the process of fusion splicing, we promote a method and also (theoretically and experimentally) prove its correctness and feasibility, using the interference among the secondary waves which are caused by reflection at the two fusion splicing points and bear end of the coupler. The method is very simple and need not require alteration of the optical configuration of the PBFOG except replacement of a conventional broad-spectrum source by a laser source having proper linewidth. Consequently, it is very helpful for process control in fabricating a high-performance PBFOG and also provides a tool to quantitatively analyze the reflection in a PBFOG.

This work was supported by the National Natural Science Foundation of China under Grant No. 61205077.

References

1. Q. Xu, Chin. Opt. Lett. **12**, S11302 (2014).
2. L. Han, L. Liu, Z. Yu, H. Zhao, X. Song, J. Mu, X. Wu, J. Long, and X. Liu, Chin. Opt. Lett. **12**, S10603 (2014).
3. F. Poletti, M. N. Petrovich, and D. J. Richardson, Nanophotonics **2**, 315 (2013).
4. K. Z. Aghaie, M. J. F. Digonnet, and S. H. Fan, J. Lightwave Technol. **31**, 1015 (2013).
5. M. Digonnet, S. Blin, H. K. Kim, V. Dangui, and G. Kino, Meas. Sci. Technol. **18**, 3089 (2007).
6. L. Olanterä, C. Sigaud, J. Troska, F. Vasey, M. N. Petrovich, F. Poletti, N. V. Wheeler, J. P. Wooler, and D. J. Richardson, in *Topical Workshop on Electronics for Particle Physics* (IOP Publishing, 2013), p. 1.
7. X. B. Xu, C. X. Zhang, and X. Pan, Optik **121**, 1170 (2010).
8. R. Thapa, K. Knabe, K. L. Corwin, and B. R. Washburn, Opt. Express **14**, 9576 (2006).
9. H. C. Lefèvre, *The Fiber-Optic Gyroscope* (Artech House, 1993).
10. A. D. Yablon, *Optical Fiber Fusion Splicing* (Springer, 2005).
11. J. Zhang, X. G. Qiao, T. Guo, Y. Y. Weng, R. H. Wang, Y. Ma, Q. Z. Rong, M. L. Hu, and Z. Y. Feng, J. Lightwave Technol. **29**, 3640 (2011).